



**VITICULTURE ORIGINAL RESEARCH ARTICLES**

# Rapid identification of boron-tolerant grapevine rootstocks via leaf spectroscopy

Yaniv Lupo<sup>1</sup>, Sadikshya Sharma<sup>1</sup>, Jose R. Munoz<sup>1</sup>, Veronica Nunez<sup>1</sup>, Ana Gaspar<sup>1</sup>, Andrew J. McElrone<sup>1,2</sup>, Luis Diaz-Garcia<sup>1,\*</sup>

<sup>1</sup> University of California, Davis, Department of Viticulture and Enology, Davis, CA 95616, USA

<sup>2</sup> USDA-ARS, Crops Pathology and Genetics Research Unit, Davis, CA 95618, USA

**Article number: 9336**



\*correspondence:  
diazgarcia@ucdavis.edu

Associate editor:  
Franco Meggio



Received:  
26 March 2025

Accepted:  
12 September 2025

Published:  
6 October 2025



This article is published under the **Creative Commons licence** (CC BY 4.0).

*Use of all or part of the content of this article must mention the authors, the year of publication, the title, the name of the journal, the volume, the pages and the DOI in compliance with the information given above.*

## ABSTRACT

Boron is an essential micronutrient for grapevine growth, yet excessive levels can impair photosynthesis, reduce yields, and diminish fruit quality. This study evaluated the potential of leaf spectroscopy combined with machine learning to identify boron-tolerant rootstocks rapidly and cost-effectively. We screened both commercial grapevine rootstocks and wild *Vitis* germplasm under boron treatments ranging from 0.5 to 8 ppm, measuring leaf boron accumulation, stomatal conductance, photosystem II efficiency, and leaf reflectance. The results revealed substantial genotypic variation in boron exclusion, with some genotypes maintaining low leaf boron concentration despite high substrate concentrations. Classification models (partial least squares discriminant analysis and random forest classification) outperformed regression models (partial least squares regression and random forest regression) in distinguishing boron-excluding genotypes, achieving 68 % to 79 % accuracy within just eight days after stress initiation. Reflectance-based vegetation indices such as the Normalized Difference Vegetation Index, Photochemical Reflectance Index, Structure Insensitive Pigment Index, and Chlorophyll Index indicated that boron stress reduces chlorophyll levels and may induce carotenoid accumulation, suggesting a photosynthetic tolerance mechanism. Although quantitative prediction of leaf boron concentration proved more challenging, simulations showed that even modest prediction accuracies (~60 %) can substantially boost genetic gains if larger populations are screened and selection intensities are increased. These findings underscore the value of leaf spectroscopy for high-throughput phenotyping, allowing breeders to rapidly identify and advance boron-tolerant rootstocks.

**KEYWORDS:** leaf spectroscopy, boron tolerance, grapevine rootstocks, high-throughput phenotyping

## INTRODUCTION

Boron (B) is an essential micronutrient that plays a crucial role in plant growth and development (Brdar-Jokanović, 2020; Brenchley & Warington, 1927; Warington, 1923). In the soil solution, B is primarily available to plants in the form of boric acid ( $H_3BO_3$ ), which is taken up by roots through passive diffusion and active transport via specific transporter proteins (Camacho-Cristóbal *et al.*, 2008). Once absorbed, B is primarily transported through the xylem via the transpiration stream, moving from the roots to the apical parts of the shoots, where it accumulates. While some plant species can also transport B through the phloem to supply low-transpiring organs (Brown & Hu, 1996; Brown & Shelp, 1997; Shelp *et al.*, 1995), it is unclear whether grapevines rely on this pathway (Blevins & Lukaszewski, 1998).

Plants require only minimal amounts of B, with an optimal soil concentration ranging between 0.5 and 2 parts per million (ppm; Botelho *et al.*, 2022). However, levels exceeding 5 ppm can lead to toxicity in many crops (Eaton, 1935; Gunes *et al.*, 2006; Oertli, 1960; Quartacci *et al.*, 2015). Boron toxicity typically manifests as reduced leaf size, chlorosis, and necrosis at the tips of mature leaves, as B accumulates in leaf tissues (Ozturk *et al.*, 2010; Princi *et al.*, 2016). In grapevines, B accumulation tends to increase with both soil B concentration and leaf age, leading to chlorosis, necrosis, reduced photosynthesis, lower stomatal conductance ( $g_s$ ), and stunted shoot growth (Pech *et al.*, 2013; Yermiyahu *et al.*, 2006). These detrimental effects underscore the importance of using B-excluding rootstocks in B-affected soils. Despite its importance, there is limited information on B tolerance in grapevines, whether among commercially available material or within wild *Vitis* germplasm. A deeper understanding of B tolerance mechanisms, the identification of tolerant germplasm, and the development of advanced breeding strategies will be critical to maintaining productivity and fruit quality in grapevine cultivation.

B concentration in leaf samples is typically estimated using either a colorimetric assay or spectrometry. In the colorimetric method, leaf tissues are first digested, usually with acids such as nitric and perchloric acid, to release B into solution. The extract is then combined with an azomethine-H reagent under acidic conditions, forming a coloured complex. The intensity of this colour, measured spectrophotometrically, is directly proportional to the B concentration in the sample (Malekani & Cresser, 1998). Alternatively, techniques such as inductively coupled plasma optical emission spectrometry (ICP-OES) or inductively coupled plasma mass spectrometry (ICP-MS) can be employed, although these methods require more specialised instrumentation (Sah & Brown, 1997). In both cases, the low throughput and elevated cost limit the screening of large sample sets typically required in breeding programmes. Furthermore, the traits related to B tolerance remain poorly understood, complicating the development of efficient screening methodologies for desirable traits such as B exclusion (Blevins & Lukaszewski, 1998).

To overcome these limitations, high-throughput phenotyping methods, which leverage proximal and remote sensing alongside algorithms for processing large, multi-dimensional datasets, are being integrated into breeding efforts to accelerate genetic gain (Araus *et al.*, 2018; Chawade *et al.*, 2019; Cohen & Alchanatis, 2018; Gao *et al.*, 2022; Singh *et al.*, 2016). Spectroscopy, in particular, has emerged as a cost-effective, non-destructive, and accurate approach for assessing key physiological traits (Sarić *et al.*, 2022). Leaf spectroscopy measures the reflectance of electromagnetic radiation from leaf tissues, which varies according to the unique spectral signatures created by different chemical bonds and organic compounds within leaves (Prananto *et al.*, 2020). The technique works by detecting how specific wavelengths are absorbed or reflected by plant tissues, with nutrients either measured directly through their incorporation in organic compounds or indirectly through correlations with spectral-active molecules.

Leaf spectroscopy has demonstrated particular success in predicting nitrogen and soluble carbohydrate content in almonds (Paz-Kagan *et al.*, 2020), chloride (Cl) content in persimmons (de Paz *et al.*, 2016), root dry matter and starch content in cassava (Hershberger *et al.*, 2022; Nkouaya Mbanjo *et al.*, 2022), disease detection in wheat (Yu *et al.*, 2018), and yield prediction in potato (Li *et al.*, 2020). In grapevines, leaf spectroscopy has been successfully applied for chloride (Cl) content (Sharma *et al.*, 2024), leaf water potential (De Bei *et al.*, 2010), and canopy nitrogen content (Walker *et al.*, 2021).

Given the limited information on how commercially available rootstocks perform under high B levels, the interactions between B accumulation and key physiological traits, and the absence of scalable, cost-effective, and time-efficient screening methods for B toxicity, this study has established two primary objectives. First, we aim to characterise B toxicity and  $g_s$  across varying stress levels in both commercial grapevine rootstocks and wild *Vitis* germplasm with breeding potential. Second, we seek to develop a spectroscopy-based methodology to predict B concentration, thereby accelerating breeding efforts. These findings provide insights into how this high-throughput strategy, even with modest prediction accuracy, can outperform traditional screening techniques in breeding programmes.

## MATERIALS AND METHODS

### 1. Plant materials

A selection of 16 genotypes, both commercial rootstocks and unreleased breeding materials from the University of California, Davis rootstock breeding programme, was evaluated. The commercial rootstocks included 140Ru (*V. berlandieri* × *V. rupestris*), 1103P (*V. berlandieri* × *V. rupestris*), 101-14Mgt (*V. riparia* × *V. rupestris*), Dog-Ridge (*V. champinii*), SO4 (*V. berlandieri* × *V. riparia*), Schwarzmann (*V. riparia* × *V. rupestris*), Riparia-Gloire (*V. riparia*), GRN3 ((Dog Ridge × Riparia

Gloire)  $\times$  *V. rufotomentosa*)  $\times$  *V. champinii*), and 110R (*V. berlandieri*  $\times$  *V. rupestris*). The breeding materials: T03-15 (*V. rupestris*), SAZ4 (*V. arizonica*), NM03-17-S01 (*V. treleasei*), Longii-9018 (*V. acerifolia*), Longii-9035 (*V. acerifolia*), 2014-160-003 (*V. acerifolia*  $\times$  Ramsey), and 2014-160-027 (*V. acerifolia*  $\times$  Ramsey); were selected based on variation in B exclusion from previous screenings in the programme.

## 2. Experimental design

The experiment was conducted in a controlled greenhouse at the University of California, Davis. The greenhouse is equipped with a pad-and-fan evaporative cooling system that activates when temperatures reach 25 °C. Hardwood cuttings (20–30 cm long and 8–12 mm diameter) were collected on 8 January 2024 and propagated. Once rooted, the cuttings were transferred into 1 L pots filled with fritted clay on 15 March 2024. Five B treatments were applied at concentrations of 0.5, 1, 2, 4, and 8 ppm. The experiment included six plants per genotype per treatment, for a total of 480 plants. B was applied through daily excess irrigation, ensuring drainage from the bottom of each pot, while all other nutrients were maintained consistently. Plants were fertigated with a complete nutrient solution containing N 150 ppm, P 50 ppm, K 200 ppm, Ca 175 ppm, Mg 55 ppm, S 120 ppm, and micronutrients (Fe 2.5, B 0.5, Mn 0.5, Zn 0.05, Cu 0.02, Mo 0.01 ppm). Treatments commenced on 7 May and concluded 29 days later, on 6 June 2024, after which leaves were harvested for B analysis.

## 3. Reflectance measurements

Leaf reflectance was measured using a CI-710s Leaf Spectrometer (CID Bio-Science, Camas, WA, USA). The CI-710s have a wavelength range of 360–1100 nm, 2.4 nm spectral resolution, and require a minimum leaf area of 10 mm  $\times$  10 mm. Measurements were taken weekly between 9:00 am and 12:00 pm on the fourth leaf from the bottom. Each leaf was measured once. White and dark reference calibrations were performed at the beginning of each measurement day using the reflectance disks provided with the CI-710s spectrometer, as specified in the manufacturer's operation manual. The raw data were preprocessed to enhance the signal-to-noise ratio as described by Hershberger *et al.* (2021) and then interpolated onto a uniform wavelength grid from  $R_{380}$  to  $R_{1100}$  nm (at 1-nm increments) using linear interpolation.

Four vegetation indices were computed from the reflectance data collected on 5 June 2024 (28 days after treatment started), as in Roberts *et al.* (2018). The Normalized Difference Vegetation Index (NDVI) was calculated as  $(\text{NIR} - \text{Red})/(\text{NIR} + \text{Red})$ , where Red reflectance was averaged over wavelengths  $R_{640}$ – $R_{670}$  nm, and NIR (Near Infrared Reflectance) was averaged over  $R_{850}$ – $R_{880}$  nm. The Photochemical Reflectance Index (PRI) was calculated as  $(R_{531} - R_{570})/(R_{531} + R_{570})$ , while the Structure Insensitive Pigment Index (SIPI) was computed as  $(R_{800} - R_{445})/(R_{800} - R_{680})$ . The Chlorophyll Index (CI) was determined

using the formula  $(\text{NIR}/\text{RedEdge}) - 1$ , where RedEdge reflectance was averaged over  $R_{700}$ – $R_{720}$  nm, and NIR was averaged the same way as for the NDVI. For each genotype-treatment combination, measurements were taken from six plants.

## 4. Boron analysis

At the end of the experiment (29 days after B treatments started), all leaves were collected, oven-dried, and sent to Davis's analytical lab at the University of California. Dry samples were ground to a fine powder, and 400 mg of each sample underwent nitric acid/hydrogen peroxide microwave digestion. The digests were then analysed by Inductively Coupled Plasma Atomic Emission Spectrometry (ICP-AES) to determine B concentration.

## 5. Physiological data

Both  $g_s$  and photosystem II efficiency ( $\Phi\text{PSII}$ ) were measured using the LI-600 Porometer/Fluorometer (LI-COR, Lincoln, NE, USA). Measurements were conducted 24 days after boron treatment initiation, with one measurement taken per leaf. The youngest, fully expanded leaf was selected from each plant, with data collected between 10:00 am and 12:00 pm. Physiological measurements were collected only for the 0.5, 4, and 8 ppm B treatments to accommodate the high number of genotype-treatment combinations and to restrict the measurement period, thereby minimising environmental variability.

## 6. Statistical analysis and modelling

The spectral data were merged with the reference lab B measurements to create a comprehensive dataset. Data cleaning involved removing extreme outliers identified via principal component analysis (PCA) on the reflectance profiles. A classification threshold of 150 ppm leaf B was used to differentiate B excluders from non-excluders, as concentrations above this level are considered toxic to grapevines (Ibacache *et al.*, 2020). Thirteen different spectral transformation methods were applied using the R package 'waves' (Hershberger *et al.*, 2021). The transformations included: standard normal variate (SNV); standard normal variate and first derivative (SNVD1); standard normal variate and second derivative (SNVD2); first derivative (D1); second derivative (D2); Savitzky–Golay with window size = 11 (SG); standard normal variate and Savitzky–Golay (SNVSG); gap segment derivative with window size = 11 (SGD1); Savitzky–Golay with window size = 5 and first derivative (SG.D1W5); Savitzky–Golay with window size = 11 and first derivative (SG.D1W11); Savitzky–Golay with window size = 5 and second derivative (SG.D2W5); Savitzky–Golay with window size = 11 and second derivative (SG.D2W11).

To predict B concentration, three different wavelength selection strategies were tested. First, prediction models were built using the full spectral range from  $R_{380}$  to  $R_{1100}$  nm. Next, highly predictive wavelengths were identified using ANOVA, with treatments and B concentration as the explanatory and response variables, respectively (Figure S1),

and variable importance projection (VIP) based on a partial least squares regression (PLS-R; Figure S2). These three feature selection approaches were then evaluated using PLS-R and random forest regression (RF-R) for quantitative prediction of B, as well as partial least squares discriminant analysis (PLS-DA) and random forest classification (RF-C) for predicting B exclusion categories based on the 150 ppm threshold. The number of trees for both RF models was 500.

In total, 156 modelling combinations were tested, representing 13 spectral transformations, 3 feature selection strategies, and 4 prediction models. For each combination, the dataset was repeatedly partitioned into training (70 %) and testing (30 %) subsets, with model performance measured as  $R^2$  (coefficient of determination) for regression or accuracy for classification, averaged over 1,000 iterations. Accuracy for classification models was calculated as the proportion of correctly classified genotypes using the formula: Accuracy = (TP + TN)/(TP + TN + FP + FN), where TP, TN, FP, and FN represent true positives, true negatives, false positives, and false negatives, respectively.

Using the AlphaSimR package (Gaynor *et al.*, 2021), we simulated responses to selection across a range of intensities and accuracies to evaluate the novel B-prediction method against traditional screening approaches. In these simulations, we assumed a genetic standard deviation of 1 and evaluated heritability levels of 0.3, 0.5, 0.7, and 0.9 across population sizes of 100, 250, 500, and 1,000 individuals. Selection intensity was varied by altering the number of individuals selected (ranging from 10 to 50), with intensity calculated as the ratio of the standard normal density at the truncation point to the selection proportion, scaled by the correlation

between phenotype and breeding value. All modelling, statistical analyses, and data visualisations were conducted using R (version 4.4.1; R Core Team, 2024).

## RESULTS

### 1. Variability in B accumulation across grapevine rootstocks

The examined rootstocks and breeding materials exhibited large variability in leaf B concentration. Two-way ANOVA revealed highly significant effects of B treatments, genotype, and their interaction on leaf B concentration ( $p < 0.001$ ; Table 1). B treatment was the strongest factor, explaining 55.5 % of the total variation, while genotype and the interaction each explained approximately 11–12 % of the variance, respectively. The leaf B concentration in T03-15 (*V. rupestris*) was 4.7 times higher than that in Longii-9035, which had the lowest levels. Across all genotypes, plants treated with 8 ppm B consistently showed a significantly higher leaf B concentration than those treated with 0.5 ppm (Figure 1A). In half of the genotypes, namely, T03-15, 140Ru, 101-14Mgt, SAZ4, Riparia-Gloire, Longii-9018, 110R, and Longii-9035, the leaf B concentration at 4 ppm was also significantly higher than at 0.5 ppm ( $p < 0.05$ ). Notably, T03-15 displayed significantly higher B levels ( $p < 0.05$ ) than all other genotypes in the 1 and 2 ppm B treatments and maintained the highest B concentration in the 4 and 8 ppm treatments (significantly higher than most of the other genotypes; Figure S3).

**TABLE 1.** Two-way ANOVA results for the effects of boron (B) treatments and genotype on leaf B concentration, stomatal conductance ( $g_s$ ), and photosystem II efficiency ( $\Phi_{PSII}$ ).

	Source	SS	df	MS	F	p	$\eta^2$
Leaf B	B	4,457,937.4	4	1,114,484.4	190.3	< 0.001	0.555
	Genotype	962,095.4	15	64,139.7	10.95	< 0.001	0.12
	Interaction	869,304.5	60	14,488.4	2.47	< 0.001	0.11
	Error	1,745,261.8	298	5,856.6			
$g_s$	B	0.45	2	0.23	13.41	< 0.001	0.081
	Genotype	1.65	15	0.11	6.52	< 0.001	0.3
	Interaction	0.32	30	0.01	0.36	0.93	0.06
	Error	3.16	187	0.02			
$\Phi_{PSII}$	B	0.2	2	0.1	5.42	0.005	0.034
	Genotype	1.62	15	0.11	5.88	< 0.001	0.28
	Interaction	0.58	30	0.02	1.05	0.4	0.1
	Error	3.42	187	0.02			

Data were analysed using two-way ANOVA with B treatment and genotype as fixed factors. Both  $g_s$  and  $\Phi_{PSII}$  were only collected in the 0.5, 4, and 8 ppm treatments. All analyses included 16 genotypes. Data were transformed when transformations improved ANOVA assumption compliance; otherwise, original data were used. SS = sum of squares; df = degrees of freedom; MS = mean square; F = F-statistic;  $\eta^2$  = eta-squared (effect size).

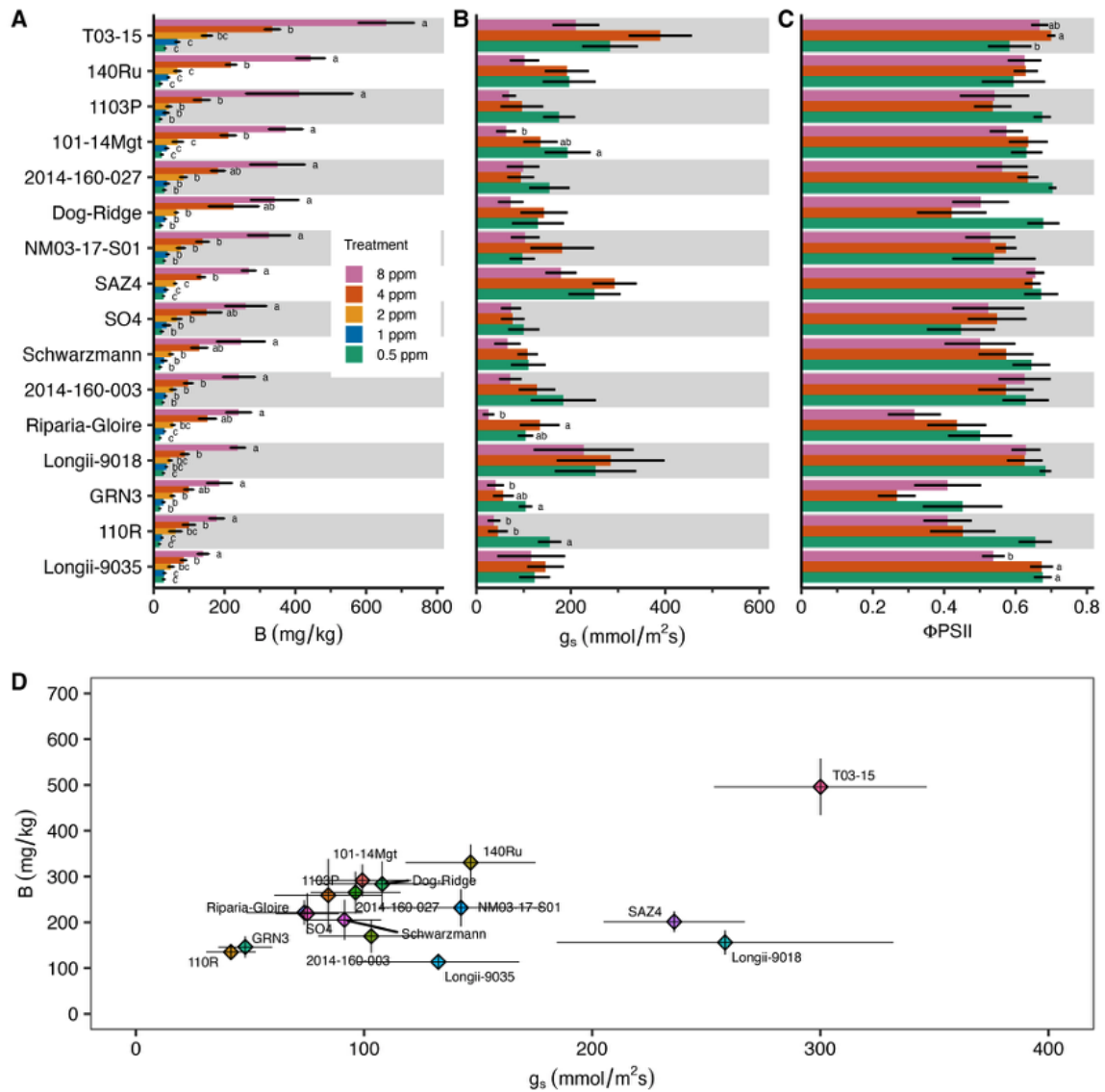


**FIGURE 1.** Leaf boron (B) concentration, stomatal conductance ( $g_s$ ), and photosystem II efficiency ( $\Phi$ PSII).

(A) Leaf B concentration, (B)  $g_s$ , and (C)  $\Phi$ PSII, ordered from highest (top) to lowest (bottom) B in the 8 ppm treatment.  $g_s$  and  $\Phi$ PSII were only collected in the 0.5, 4, and 8 ppm treatments. Bars represent the mean  $\pm$  standard error. (D) B vs  $g_s$  for the 4 and 8 ppm treatments; horizontal and vertical bars represent the mean  $\pm$  standard error for each variable. Different letters denote significant differences among treatments within each genotype (one-way ANOVA followed by Tukey HSD,  $p < 0.05$ ). If no letters appear for a given genotype, there were no significant differences among treatments for that genotype.

## 2. Physiological responses and relationship with leaf B concentration

Two-way ANOVA revealed significant effects of both B and genotype on  $g_s$  and  $\Phi$ PSII (Table 1). Genotype explained the largest proportion of variance ( $g_s = 30\%$ ,  $\Phi$ PSII = 28%), while B treatment accounted for 8.1% ( $g_s$ ) and 3.4% ( $\Phi$ PSII) of the total variation. Overall, there was no correlation between the  $g_s$  and B ( $r = 0.049$ ,  $p = 0.4$ ). However, three genotypes, 101-14Mgt, GRN3, and 110R (commercial rootstocks), exhibited a significant reduction in  $g_s$  between the 8 ppm and 0.5 ppm treatments ( $p < 0.05$ ; Figure 1B). In contrast, Longii-9035 and Longii-9018 maintained stable  $g_s$  values across all treatments. There was no correlation between  $\Phi$ PSII and B ( $r = 0.01$ ,  $p = 0.06$ ); while some genotypes experienced reductions between 1.36% and 37.5% (110R)

in the 8 ppm treatment compared to 0.5 ppm, others showed no change or even an increase of 2.77–14.42% (Figure 1C). Notably, Longii-9035 was the only genotype that demonstrated a significant decline in  $\Phi$ PSII in the 8 ppm treatment relative to the 0.5 ppm treatment ( $p < 0.05$ ).

When comparing leaf B concentration against  $g_s$ , most genotypes clustered together, with several genotypes either over- or under-performing relative to the cluster (Figure 1D). T03-15, for example, had both the highest leaf B and  $g_s$ , whereas Longii-9035 exhibited the lowest leaf B and an intermediate  $g_s$ . Additionally, GRN3 and 110R formed a distinct cluster with relatively low values for both parameters, while SAZ4 and Longii-9018 clustered together with low leaf B yet maintained high  $g_s$ .

### 3. Analysis of vegetation indices in response to B

Leaf NDVI reduced in response to elevated B levels compared to the 0.5 ppm treatment, with significant reductions in the 2 and 4 ppm treatments ( $p < 0.05$ ; Figure 2A). PRI, which reflects changes in photosynthetic light-use efficiency, also had a reduction trend in response to elevated B levels, with a significant reduction in the 4 ppm treatment ( $p < 0.05$ ; Figure 2B). The SIPI, which provides insights on the balance between carotenoids and chlorophyll, decreased in the 2 and 4 ppm treatments, compared to the 0.5 ppm treatment, but not in the 1 and 8 ppm treatments

(Figure 2C). The CI decreased in the 1, 2, and 4 ppm treatments compared to the 0.5 ppm treatment, but not in the 8 ppm which was also higher than the 2 and 4 ppm treatments (Figure 2D). The genotypes had different NDVI, PRI, SIPI, and CI responses to the B treatments. Notably, Longii-9035 had similar values of NDVI in all the treatments (Figure 2E). Longii-9035 also had similar or higher values of PRI, SIPI, and CI in the 8 ppm treatment compared to the 0.5 ppm treatment (Figures 2F, 2G and 2H). Leaf B concentration did not correlate with any of the four vegetative indices (NDVI, PRI, CI, and SIPI; Figure S4).

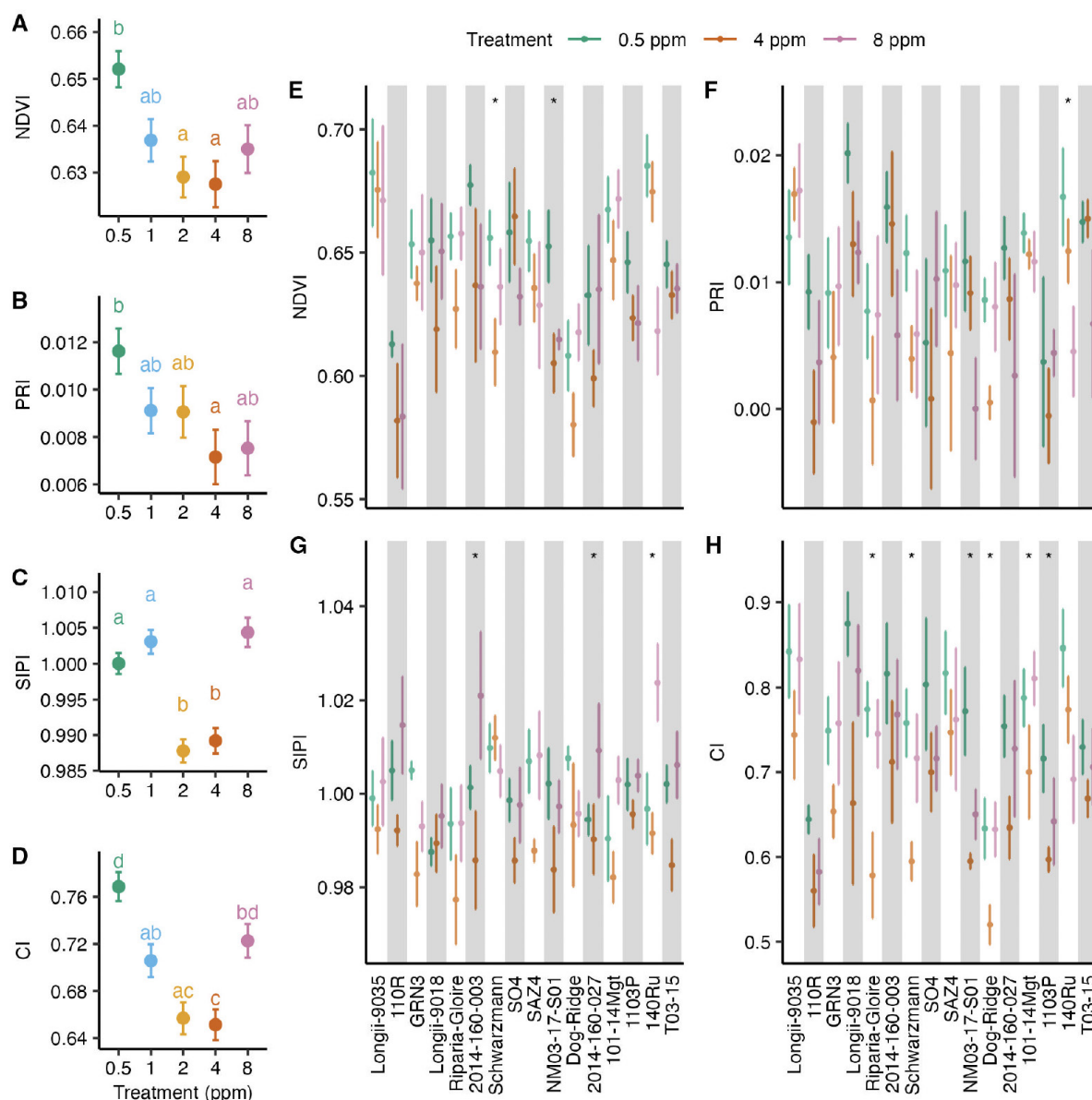


**FIGURE 2.** Vegetation indices derived from reflectance measurements.

(A) Normalized Difference Vegetation Index (NDVI) by treatment. (B) Photochemical Reflectance Index (PRI) by treatment. (C) Structure Insensitive Pigment Index (SIPI) by treatment. (D) Chlorophyll Index (CI) by treatment. (E) NDVI by treatment and by genotype. (F) PRI by treatment and by genotype. (G) SIPI by treatment and by genotype. (H) CI by treatment and by genotype. Points represent the mean index values with corresponding standard errors. Different letters denote significant differences among treatments (one-way ANOVA followed by Tukey HSD,  $p < 0.05$ ). Asterisks denote significant differences among treatments within each genotype (one-way ANOVA,  $p < 0.05$ ).

#### 4. Spectral data processing, wavelength selection, and model development

Reflectance across most of the visible (VIS) spectrum ( $\sim R_{500}$ – $R_{700}$  nm) increased with B levels, showing the lowest reflectance in the 0.5 ppm treatment and the highest in the 8 ppm treatment (Figure 3B). However, this pattern did not hold in the NIR region ( $\sim R_{750}$ – $R_{1100}$  nm), where the lowest (0.5 ppm) and highest (8 ppm) treatments exhibited higher reflectance than the intermediate treatments (1, 2, and 4 ppm; Figure 3A). One-way ANOVAs performed separately for each wavelength revealed significant differences among the B treatments for most of the examined spectral range ( $\sim R_{475}$ – $R_{520}$  nm and above  $R_{600}$  nm;  $p < 0.05$ ; Figure 3C). Examination of VIP scores calculated from a PLS-R model revealed a different pattern, where VIP scores greater than 1, indicative of high predictive relevance, occurred mostly at the edges of the spectrum, including a notable peak at the edge of the VIS region ( $\sim R_{630}$ – $R_{760}$  nm; Figure 3D).

#### 5. Evaluation of regression and classification models for the prediction of leaf B

We observed clear performance differences between models predicting B concentrations (PLS-R and RF-R) and those classifying B exclusion categories (PLS-DA and RF-C). PLS-R and RF-R exhibited consistently lower accuracy ( $\sim 0.1$  to  $0.4$ ) regardless of the wavelength selection strategy (using all wavelengths, or selecting wavelengths based on ANOVA or VIP) and the spectral transformation method applied (Figures 4A and 4B). In contrast, models focused on categorical prediction, PLS-DA and RF-C, achieved substantially higher accuracy ( $\sim 0.6$  to  $0.8$ ), suggesting that spectral data are more effective at distinguishing B-excluding genotypes than at precisely quantifying B concentrations (Figures 4C and 4D).

Across all models, the choice of wavelength selection method had minimal impact on performance, with accuracy remaining relatively stable whether all wavelengths were used or features were selected via ANOVA or VIP.

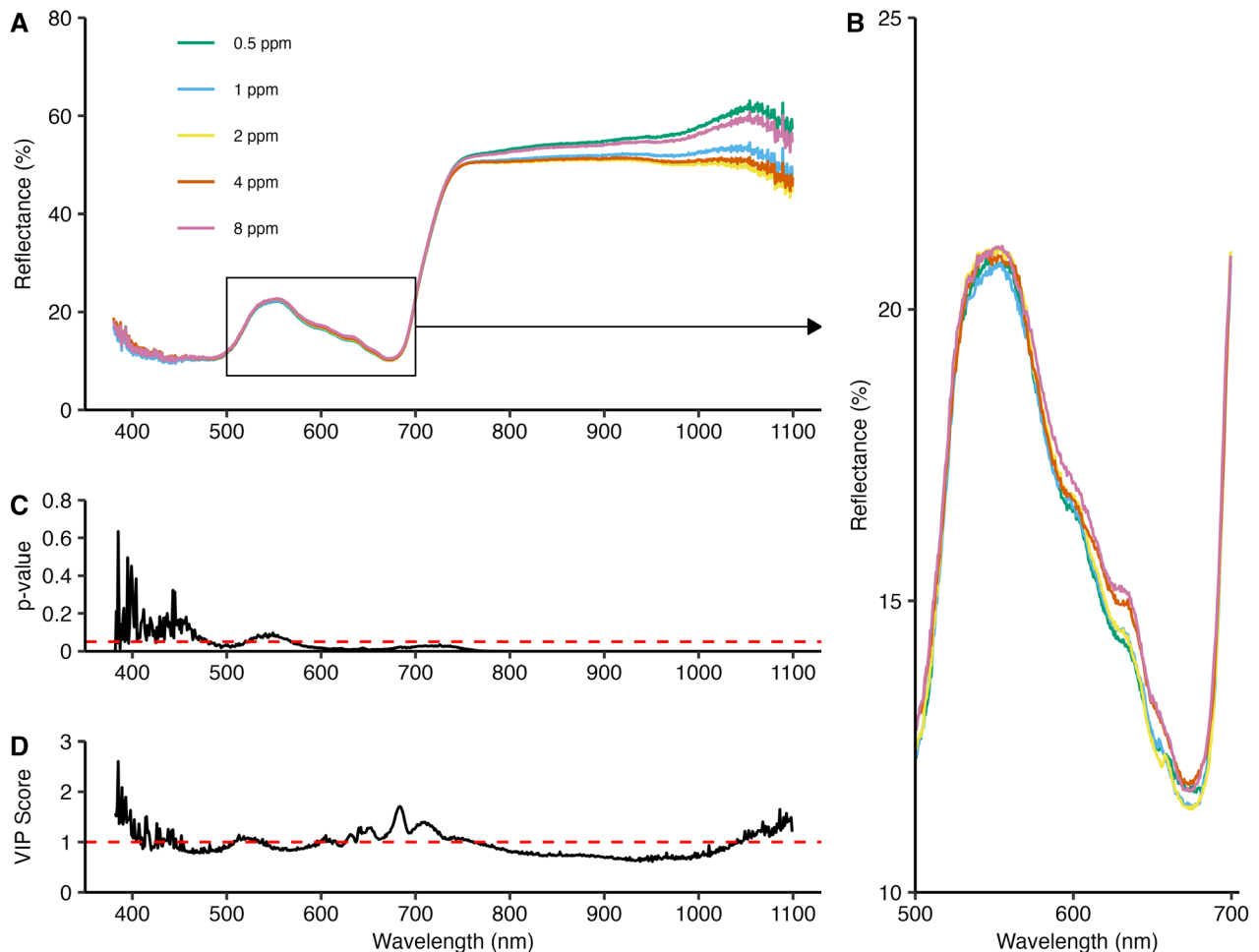


**FIGURE 3.** Raw reflectance and results of the ANOVA and variable importance projection (VIP) based selection criteria.

(A) Raw reflectance for each of the B treatments. Each line is the mean of all the plants from one treatment. (B) Raw reflectance for each B treatment at wavelengths between 500–700 nm. Each line is the mean of all the plants from one treatment. (C)  $p$ -values from one-way ANOVAs between the B treatment within each wavelength. Wavelengths with  $p < 0.05$  (below the red dotted line) were selected for prediction. (D) VIP scores calculated from a preliminary PLS model between the raw reflectance data and the measured B. Wavelengths with  $VIP > 1$  (above the red dotted line) were selected for prediction.

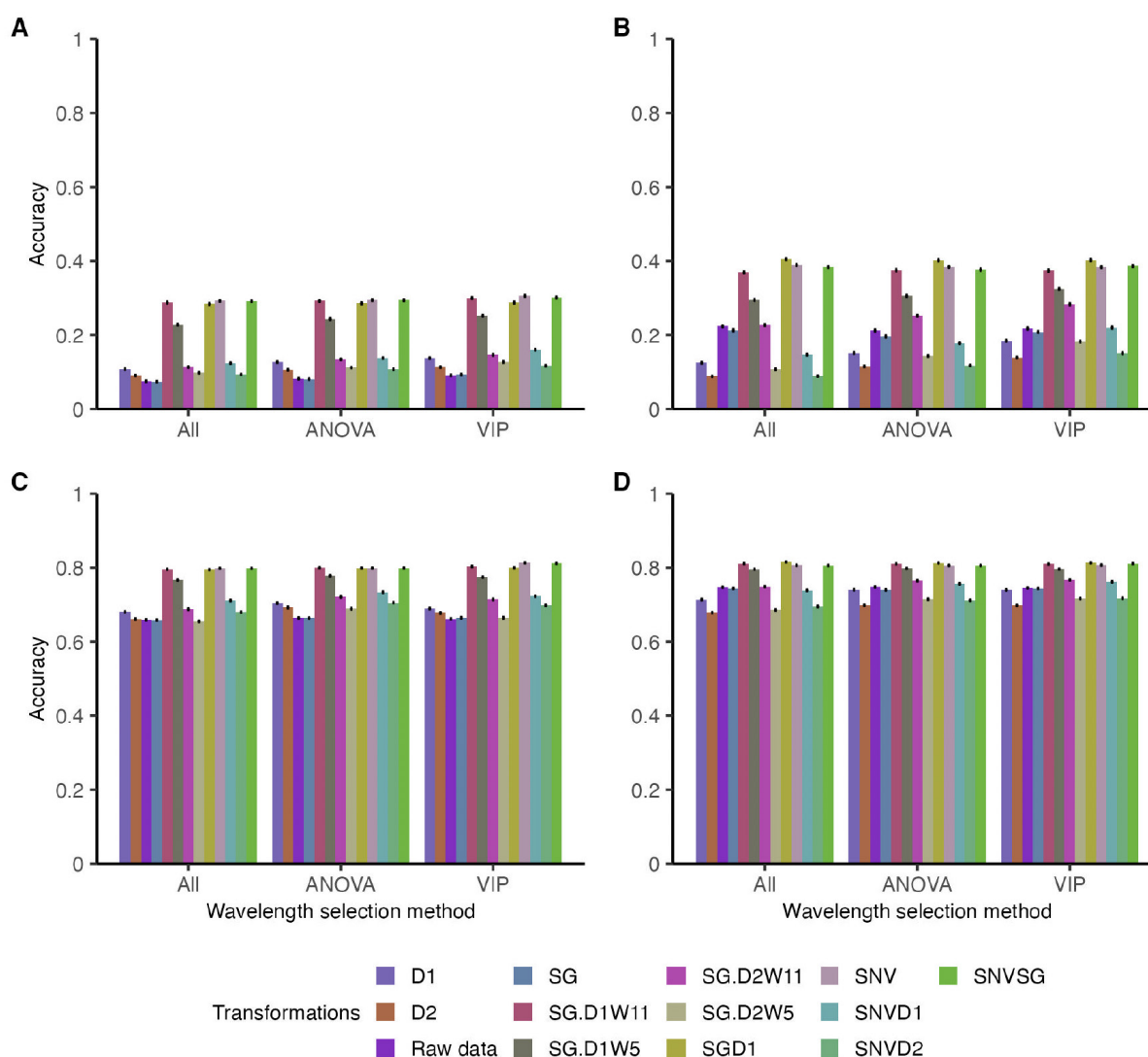


**FIGURE 4.** Performance accuracies of boron (B) prediction models for different wavelength selection strategies and transformation methods.

(A) Partial least squares regression (PLSR). (B) Random forest regression model (RF-R). (C) Partial least squares discriminant analysis (PLS-DA). (D) Random forest classification model (RF-C). Models are compared under three wavelength-selection criteria: all, using all available wavelengths; ANOVA, using only wavelengths with  $p < 0.05$  from an ANOVA between treatments; VIP, using only wavelengths with VIP score  $> 1$  from a PLSR model. For each combination, different colours represent different reflectance transformations. Each bar shows the mean performance accuracy over 1,000 iterations of each model. Error bars indicate the standard errors of the mean. For PLSR and RF regression, performance is reported as  $R^2$ ; for the PLS-DA and RF classification models, accuracy corresponds to classification performance. Measurements were taken after 29 days of treatment.

Similarly, the spectral transformation method did not produce large deviations in accuracy, though some transformations, such as SGD1, SNV, and SNVSG, tended to yield slightly better performance in PLS-DA and RF-C.

To assess the potential for early B prediction and classification, we applied similar modelling approaches to reflectance data collected eight days after treatments began (Figure 5). These models followed the same methodology as those used for the final reflectance measurements (Figure 4). As observed with the final measurements, regression models had lower accuracy than classification models. Among

the regression approaches, PLS-R showed the poorest performance, with a maximum  $R^2$  of 0.21 (Figure 5A), whereas RF-R performed slightly better, reaching a maximum  $R^2$  of 0.34 (Figure 5B). Compared to the final reflectance measurement, PLS-R had a similar range of low accuracy, while RF-R had a slightly lower average  $R^2$  in the early measurement (0.11) than in the final measurement (0.26, Figure 4C). However, the best-performing RF-R model using early measurement data (SNV, all wavelengths,  $R^2 = 0.34$ ) showed comparable accuracy to the best RF-R model from the final measurement (SGD1, all wavelengths,  $R^2 = 0.4$ ; Figure 5C).

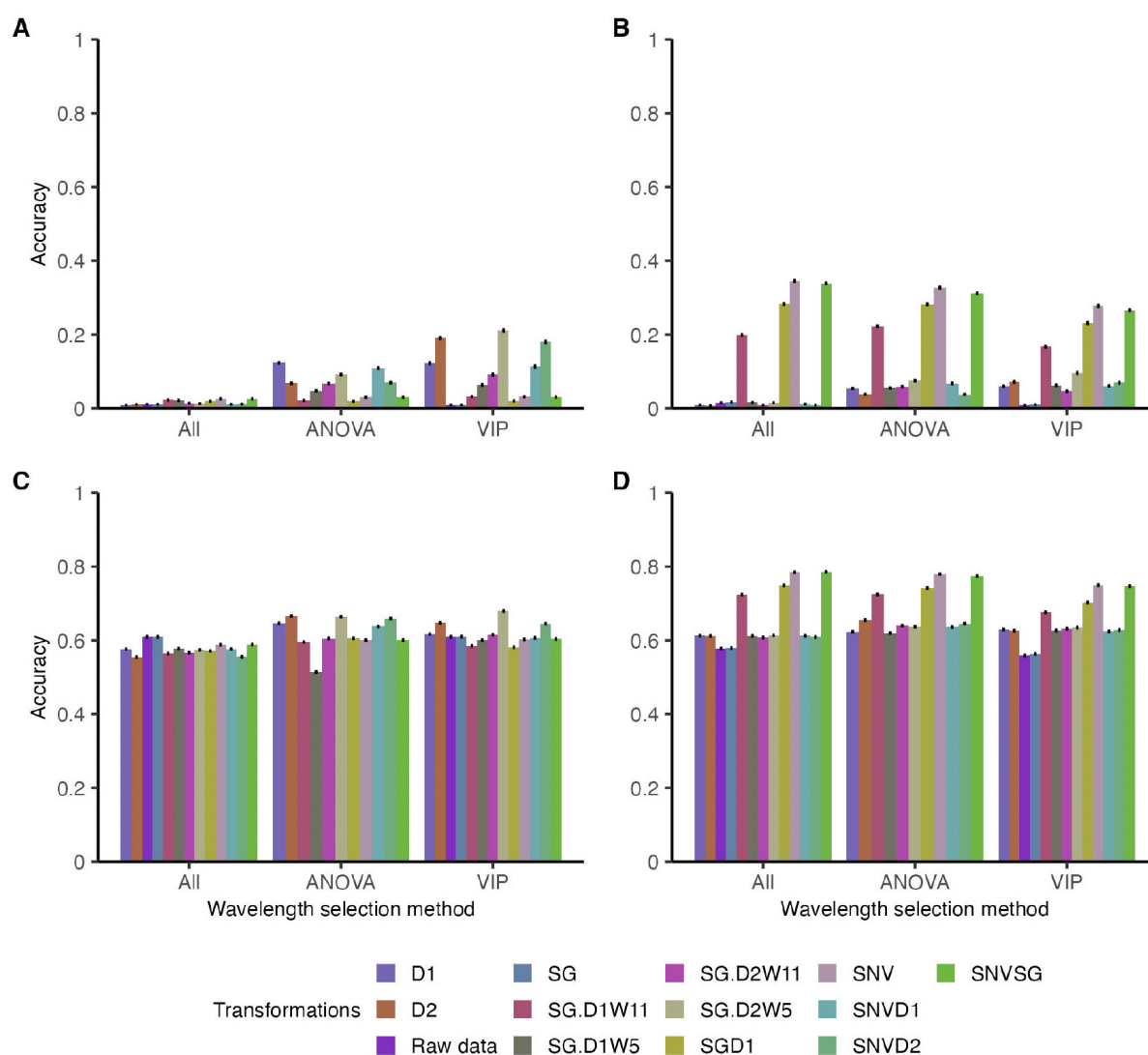


**FIGURE 5.** Performance accuracies of boron (B) prediction models after eight days of B treatment.

(A) Partial least squares regression (PLS-R). (B) Random forest regression model (RF-R). (C) Partial least squares discriminant analysis (PLS-DA). (D) Random forest classification model (RF-C). Models' methodologies are explained in Figure 4 and in the "Materials and methods". For PLS-R and RF-R, performance is reported as  $R^2$ ; for the PLS-DA and RF-C models, accuracy corresponds to classification performance. Measurements were taken after eight days of treatment.

For classification models, PLS-DA performed worse with early measurement data, achieving a maximum accuracy of 0.68 (Figure 5B), compared to 0.81 in the final measurement (Figure 4B). RF-C also showed a drop in accuracy, with an early measurement average of 0.66 (Figure 5D) compared to 0.82 in the final measurement (Figure 4D). However, SNVSG and SNV transformations maintained relatively stable performance in PLS-DA, with early measurement accuracies of 0.79 and 0.78, respectively, compared to 0.81 for both transformations in the final measurement. These results indicate that while early spectral measurements can capture some variation in B concentration, classification models remain more reliable than regression models for early B prediction.

## DISCUSSION

The significant interaction effect between B treatments and genotype on leaf B concentration (Table 1) indicates that genotypes examined differ in their B accumulation patterns across B levels. The genotypes exhibited large variation in leaf B exclusion, which has the potential for breeding new B-tolerant rootstocks. Contrary to expectations, there was no correlation between  $g_s$  and leaf B concentration (Figure S5). Since B is primarily transported to the shoots via the xylem stream (Pereira *et al.*, 2021), we anticipated that higher  $g_s$  would lead to increased B translocation and accumulation in the leaves. T03-15, which had the highest leaf B concentration, also exhibited the highest  $g_s$ , while GRN3 and 110R, which had relatively low B concentration, showed the

lowest  $g_s$ . Among the genotypes with low leaf B, SAZ4 and Longii-9018 maintained relatively high  $g_s$ , suggesting that their lower B concentration may be due to active B exclusion mechanisms rather than reduced transpiration. These exclusion mechanisms could involve reduced B uptake from the soil or enhanced B removal from the shoot (Brown & Hu, 1996; Miwa *et al.*, 2007; Wakuta *et al.*, 2016) and might involve aquaporins (Mosa *et al.*, 2016).

Boron and Cl stresses share similarities, as both ions function as micronutrients but become toxic at high concentrations (Munns & Tester, 2008). However, B and Cl differ in their toxic threshold concentrations and mobility within the plant, as B is generally considered less mobile than Cl (Brown & Shelp, 1997; White & Broadley, 2001). Previous studies have identified a combined response to B and Cl stress in grapevines (Ben-Gal *et al.*, 2008; Downton & Hawker, 1980) and *Prunus* rootstocks (El-Motaium *et al.*, 1994). Notably, Longii-9035 and Longii-9018, which exhibited low B accumulation, also demonstrated enhanced Cl exclusion capacities (Sharma *et al.*, 2024). The ability of these genotypes to exclude both B and Cl under high concentrations suggests that a shared physiological mechanism may be involved. These findings underscore their potential as valuable candidates for future breeding programmes aimed at developing rootstocks with combined B and Cl tolerance.

The observed increase in reflectance in the VIS range at higher B levels (Figure 3B) suggests that elevated B concentrations reduce light absorption by the leaves. This effect may be linked to decreased photosynthetic activity due to B toxicity, which can reduce chlorophyll concentration or increase carotenoid accumulation (Landi *et al.*, 2013). However, this trend did not persist in the VNIR range, where the lowest (0.5 ppm) and highest (8 ppm) B treatments exhibited higher reflectance than the intermediate treatments (1, 2, and 4 ppm). One possible explanation for the 8 ppm treatment is that excessive B accumulates in the mesophyll cell wall, leading to denser cell walls that reduce light absorption in the VNIR range (Ozturk *et al.*, 2010). Previously, high concentrations of B were found to change functional groups in rice leaves' cell walls, such as the methine group (-CH), which affects the structural and functional roles of cellulose and pectin (Riaz *et al.*, 2021).

Leaf spectroscopy combined with machine learning is a promising approach for large-scale, cost-effective, and time-efficient B classification, as demonstrated by the results. Classification models for B excluders demonstrated strong potential, achieving 68 % to 79 % accuracy even within a few days of stress initiation. This would offer a practical solution for screening plant material in breeding programmes, especially when phenotyping is a bottleneck. Similar results were found in the classification of virus infection in grapevines using hyperspectral sensing (Wang *et al.*, 2023). In contrast, quantitative B prediction was less reliable, with regression models achieving maximum  $R^2$  values of 0.4. These findings align with previous research showing that micronutrient concentrations, including B, are more challenging to predict from hyperspectral data than

macronutrients (Grieco *et al.*, 2022; Pandey *et al.*, 2017). In fact, Pandey *et al.* (2017) identified B as one of the least predictable elements. Similarly, Sharma *et al.* (2024) found that classification models were more effective than regression models for predicting Cl exclusion in grapevines using spectral data, suggesting that categorical approaches may be more robust for ion exclusion studies.

The observed reductions in NDVI and PRI with increasing B concentration in the irrigation solution suggest a decline in photosynthesis, possibly due to chlorophyll loss (Gitelson & Merzlyak, 1997) or reduced light-use efficiency (Gamon *et al.*, 1992). The reduction in CI (Figure 2D) further supports the idea that NDVI declines were driven by reduced chlorophyll concentration (Gitelson & Merzlyak, 1994). Although these indices are not specific to B toxicity and may be influenced by other environmental or physiological factors, the consistent decline with increasing B supports their utility as indicators of stress-induced changes in photosynthetic function. Interestingly, SIPI followed a different trend, decreasing at 2 and 4 ppm but not at 8 ppm. This distinct response may indicate increased carotenoid accumulation in the leaves, as suggested by Penuelas *et al.* (1995). The differences in SIPI and CI patterns between the 2 and 4 ppm treatments *versus* the 8 ppm treatment suggest that at high B concentrations, carotenoid accumulation may serve as a protective mechanism against B-induced stress, a phenomenon observed under other stress conditions as well (Uarrotta *et al.*, 2018). While  $\Phi$ PSII was not significantly affected, these findings suggest that B stress may negatively impact photosynthesis indirectly, potentially through pigment degradation or altered light-use efficiency, and that carotenoid accumulation may contribute to B toxicity tolerance. This insight could help identify genotypes with improved B stress resilience, informing future breeding efforts for B-tolerant rootstocks.

Moderate accuracies (*e.g.*, 0.5–0.6) may limit the appeal of spectroscopy-based methods for certain breeding applications. However, in a breeding context, particularly when considering response to selection, lower accuracies can be offset by larger population sizes and higher selection intensities. To explore this potential, we simulated how different population sizes, selection intensities, and heritabilities affect the response to selection ( $R$ ; Figure 6). The results follow expected patterns:  $R$  increases with rising heritability and greater selection intensity. By removing the phenotyping bottleneck, for instance, through cost-effective, high-throughput spectroscopy, breeders can expand their screening capacity from 100 to 500 individuals. Under these conditions, tripling the selection intensity from 10 to 30 individuals increases  $R$  from about 1.5 to 2, reflecting roughly a 33 % improvement in genetic gain. Although these simulations are primarily illustrative and do not account for detailed cost analyses of different screening technologies, they highlight how increasing population size and adjusting selection intensity can substantially boost the response to selection.

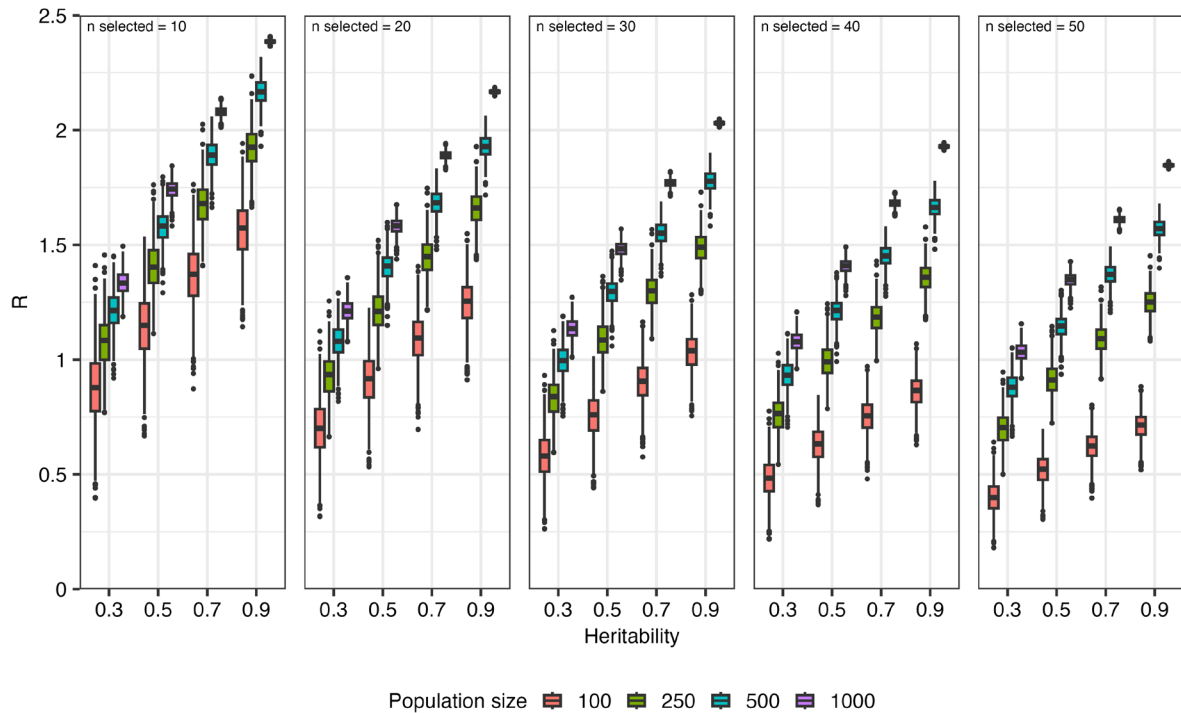


**FIGURE 6.** Response to selection ( $R$ ) as a function of heritability, population size, and selection intensity.

Boxplots display the distribution of the simulated genetic response ( $R$ ) across four heritability levels (0.3, 0.5, 0.7, and 0.9) for four population sizes (100, 250, 500, and 1,000 individuals) over 1,000 iterations. Each panel corresponds to a fixed number of individuals selected ( $n$  selected), with the selection intensity calculated as the ratio of the standard normal density at the truncation point to the selection proportion, multiplied by the correlation between phenotype and breeding value, and a genetic standard deviation of 1. Different colours indicate the distinct population sizes.

## CONCLUSIONS

This study highlights the substantial variation in leaf B concentration across different *Vitis* genotypes, demonstrating clear opportunities to breed new B-tolerant rootstocks. Although we initially expected a link between  $g_s$  and leaf B concentration, no such correlation emerged, suggesting that active exclusion mechanisms may play a larger role than transpiration-driven processes in controlling B accumulation. Notably, several genotypes (e.g., Longii-9018, Longii-9035, SAZ4) combined low B accumulation with robust physiological performance, and some even showed improved CI exclusion, hinting at a shared mechanism for multi-ion tolerance. These findings also show that leaf spectroscopy integrated with machine learning can effectively classify B-excluding genotypes, offering a scalable, cost-effective, and time-efficient plant phenotyping approach. While regression models for quantitative B prediction remain less reliable, classification models proved sufficiently accurate for early screening, critical for breeding programmes where phenotyping is often a bottleneck. Moreover, simulation results indicate that moderate predictive accuracies can still drive substantial genetic gain if population size and selection intensities are increased. By removing or reducing the phenotyping bottleneck, breeders can more readily exploit genetic diversity for B tolerance, accelerating the development of robust, multi-stress-tolerant rootstocks that maintain productivity under high B and other abiotic stresses.

## ACKNOWLEDGEMENTS

The authors would like to thank Mikayla Bailey, Guillermo Garcia-Zamora, and Patrick H. Brown for their support and valuable recommendations in the execution of this work. This research was supported by BARD, the United States–Israel Binational Agricultural Research and Development Fund, Vaadia-BARD Postdoctoral Fellowship Award No FI-633-2023, and the USDA National Institute of Food and Agriculture Specialty Crop Research Initiative (awards 2022-51181-38240 and 2024-51181-43236).

## REFERENCES

- Araus, J. L., Kefauver, S. C., Zaman-Allah, M., Olsen, M. S., & Cairns, J. E. (2018). Translating high-throughput phenotyping into genetic gain. *Trends in Plant Science*, 23(5), 451–466. <https://doi.org/10.1016/j.tplants.2018.02.001>
- Ben-Gal, A., Yermiyahu, U., Shani, U., & Veste, M. (2008). Irrigating table grapes in arid regions with low quality water: Effects of salinity and excess boron. *Acta Horticulturae*, 792, 107–114. <https://doi.org/10.17660/ActaHortic.2008.792.10>
- Blevins, D. G., & Lukaszewski, K. M. (1998). Boron in plant structure and function. *Annual Review of Plant Physiology and Plant Molecular Biology*, 49(1), 481–500. <https://doi.org/10.1146/annurev.arplant.49.1.48>

- Botelho, R. V., Müller, M. M. L., Umburanas, R. C., Laconski, J. M. O., & Terra, M. M. (2022). Chapter 2 - Boron in fruit crops: Plant physiology, deficiency, toxicity, and sources for fertilization. In T. Aftab, M. Landi, I. E. Papadakis, F. Araniti, & P. Brown (Eds.), *Boron in Plants and Agriculture*. Academic Press. <https://doi.org/10.1016/B978-0-323-90857-3.00015-1>
- Brdar-Jokanović, M. (2020). Boron toxicity and deficiency in agricultural plants. *International Journal of Molecular Sciences*, 21(4). <https://doi.org/10.3390/ijms21041424>
- Brenchley, W. E., & Warington, K. (1927). The role of boron in the growth of plants. *Annals of Botany*, 41(161), 167–187. <https://doi.org/10.1093/oxfordjournals.aob.a090062>
- Brown, P. H., & Hu, H. (1996). Phloem mobility of boron is species dependent: Evidence for phloem mobility in sorbitol-rich species. *Annals of Botany*, 77(5), 497–506. <https://doi.org/10.1006/anbo.1996.0060>
- Brown, P. H., & Shelp, B. J. (1997). Boron mobility in plants. *Plant and Soil*, 193(1), 85–101. <https://doi.org/10.1023/A:1004211925160>
- Camacho-Cristóbal, J. J., Rexach, J., & González-Fontes, A. (2008). Boron in plants: Deficiency and toxicity. *Journal of Integrative Plant Biology*, 50(10), 1247–1255. <https://doi.org/10.1111/j.1744-7909.2008.00742.x>
- Chawade, A., van Ham, J., Blomquist, H., Bagge, O., Alexandersson, E., & Ortiz, R. (2019). High-throughput field-phenotyping tools for plant breeding and precision agriculture. *Agronomy*, 9(5), Article 5. <https://doi.org/10.3390/agronomy9050258>
- Cohen, Y., & Alchanatis, V. (2018). Spectral and spatial methods for hyperspectral and thermal image-analysis to estimate biophysical and biochemical properties of agricultural crops. In P. S. Thenkabail, J. G. Lyon, & A. Huete (Eds.), *Biophysical and Biochemical Characterization and Plant Species Studies* (2nd ed., pp. 73–101). CRC Press. <https://doi.org/10.1201/9780429431180-3>
- De Bei, R., Cozzolino, D., Sullivan, W., Cynkar, W., Fuentes, S., Damberg, R., Pech, J., & Tyerman, S. (2010). Non-destructive measurement of grapevine water potential using near infrared spectroscopy. *Australian Journal of Grape and Wine Research*, 17, 62–71. <https://doi.org/10.1111/j.1755-0238.2010.00117.x>
- de Paz, J. M., Visconti, F., Chiaravalle, M., & Quiñones, A. (2016). Determination of persimmon leaf chloride contents using near-infrared spectroscopy (NIRS). *Analytical and Bioanalytical Chemistry*, 408(13), 3537–3545. <https://doi.org/10.1007/s00216-016-9430-2>
- Downton, W. J. S., & Hawker, J. S. (1980). Interaction of boron and chloride on growth and mineral composition of Cabernet Sauvignon vines. *American Journal of Enology and Viticulture*, 31(3), 277–282. <https://doi.org/10.5344/ajev.1980.31.3.277>
- Eaton, F. M. (1935). Boron in soils and irrigation waters and its effect on plants. *Technical Bulletin*, 448.
- El-Motaium, R., Hu, H., & Brown, P. H. (1994). The relative tolerance of six *prunus* rootstocks to boron and salinity. *Journal of the American Society for Horticultural Science*, 119(6), 1169–1175. <https://doi.org/10.21273/JASHS.119.6.1169>
- Gamon, J. A., Peñuelas, J., & Field, C. B. (1992). A narrow-waveband spectral index that tracks diurnal changes in photosynthetic efficiency. *Remote Sensing of Environment*, 41(1), 35–44. [https://doi.org/10.1016/0034-4257\(92\)90059-S](https://doi.org/10.1016/0034-4257(92)90059-S)
- Gao, R., Torres-Rua, A. F., Aboutalebi, M., White, W. A., Anderson, M., Kustas, W. P., Agam, N., Alsina, M. M., Alfieri, J., Hipps, L., Dokoozlian, N., Nieto, H., Gao, F., McKee, L. G., Prueger, J. H., Sanchez, L., Mcelrone, A. J., Bambach-Ortiz, N., Coopmans, C., & Gowing, I. (2022). LAI estimation across California vineyards using sUAS multi-seasonal multi-spectral, thermal, and elevation information and machine learning. *Irrigation Science*, 40(4), 731–759. <https://doi.org/10.1007/s00271-022-00776-0>
- Gaynor, R. C., Gorjanc, G., & Hickey, J. M. (2021). AlphaSimR: An R package for breeding program simulations. *G3 Genes|Genomes|Genetics*, 11(2), jkaa017. <https://doi.org/10.1093/g3journal/jkaa017>
- Gitelson, A. A., & Merzlyak, M. N. (1997). Remote estimation of chlorophyll content in higher plant leaves. *International Journal of Remote Sensing*, 18(12), 2691–2697. <https://doi.org/10.1080/014311697217558>
- Gitelson, A., & Merzlyak, M. N. (1994). Spectral reflectance changes associated with autumn senescence of *Aesculus hippocastanum* L. and *Acer platanoides* L. leaves. Spectral features and relation to chlorophyll estimation. *Journal of Plant Physiology*, 143(3), 286–292. [https://doi.org/10.1016/S0176-1617\(11\)81633-0](https://doi.org/10.1016/S0176-1617(11)81633-0)
- Grieco, M., Schmidt, M., Warnemünde, S., Backhaus, A., Klück, H.-C., Garibay, A., Tandrón Moya, Y. A., Jozefowicz, A. M., Mock, H.-P., Seiffert, U., Maurer, A., & Pillen, K. (2022). Dynamics and genetic regulation of leaf nutrient concentration in barley based on hyperspectral imaging and machine learning. *Plant Science*, 315, 111123. <https://doi.org/10.1016/j.plantsci.2021.111123>
- Gunes, A., Soylemezoglu, G., Inal, A., Bagci, E. G., Coban, S., & Sahin, O. (2006). Antioxidant and stomatal responses of grapevine (*Vitis vinifera* L.) to boron toxicity. *Scientia Horticulturae*, 110(3), 279–284. <https://doi.org/10.1016/j.scienta.2006.07.014>
- Hershberger, J., Mbanjo, E. G. N., Peteti, P., Ikpan, A., Ogunpaimo, K., Nafiu, K., Rabbi, I. Y., & Gore, M. A. (2022). Low-cost, handheld near-infrared spectroscopy for root dry matter content prediction in cassava. *The Plant Phenome Journal*, 5(1), e20040. <https://doi.org/10.1002/ppj2.20040>
- Hershberger, J., Morales, N., Simoes, C. C., Ellerbrock, B., Bauchet, G., Mueller, L. A., & Gore, M. A. (2021). Making waves in Breedbase: An integrated spectral data storage and analysis pipeline for plant breeding programs. *The Plant Phenome Journal*, 4(1), e20012. <https://doi.org/10.1002/ppj2.20012>
- Ibacahe, A., Verdugo-Vásquez, N., & Zurita-Silva, A. (2020). Rootstock: Scion combinations and nutrient uptake in grapevines. In *Fruit Crops* (pp. 297–316). Elsevier. <https://doi.org/10.1016/B978-0-12-818732-6.00021-6>
- Landi, M., Remorini, D., Pardossi, A., & Guidi, L. (2013). Boron excess affects photosynthesis and antioxidant apparatus of greenhouse Cucurbita pepo and Cucumis sativus. *Journal of Plant Research*, 126(6), 775–786. <https://doi.org/10.1007/s10265-013-0575-1>
- Li, B., Xu, X., Zhang, L., Han, J., Bian, C., Li, G., Liu, J., & Jin, L. (2020). Above-ground biomass estimation and yield prediction in potato by using UAV-based RGB and hyperspectral imaging. *ISPRS Journal of Photogrammetry and Remote Sensing*, 162, 161–172. <https://doi.org/10.1016/j.isprsjprs.2020.02.013>
- Malekani, K., & Cresser, M. S. (1998). Comparison of three methods for determining boron in soils, plants, and water samples. *Communications in Soil Science and Plant Analysis*, 29(3–4), 285–304. <https://doi.org/10.1080/00103629809369946>
- Miwa, K., Takano, J., Omori, H., Seki, M., Shinozaki, K., & Fujiwara, T. (2007). Plants tolerant of high boron levels. *Science*, 318(5855), 1417–1417. <https://doi.org/10.1126/science.1146634>

- Mosa, K. A., Kumar, K., Chhikara, S., Musante, C., White, J. C., & Dhankher, O. P. (2016). Enhanced boron tolerance in plants mediated by bidirectional transport through plasma membrane intrinsic proteins. *Scientific Reports*, 6(1), Article 1. <https://doi.org/10.1038/srep21640>
- Munns, R., & Tester, M. (2008). Mechanisms of salinity tolerance. *Annual Review of Plant Biology*, 59(1), 651–681. <https://doi.org/10.1146/annurev.arplant.59.032607.092911>
- Nkouaya Mbanjo, E. G., Hershberger, J., Peteti, P., Agbona, A., Ikpan, A., Ogunpaimo, K., Kayondo, S. I., Abioye, R. S., Nafiu, K., Alamu, E. O., Adesokan, M., Maziya-Dixon, B., Parkes, E., Kulakow, P., Gore, M. A., Egesi, C., & Rabbi, I. Y. (2022). Predicting starch content in cassava fresh roots using near-infrared spectroscopy. *Frontiers in Plant Science*, 13. <https://doi.org/10.3389/fpls.2022.990250>
- Oertli, J. J. (1960). The distribution of normal and toxic amounts of boron in leaves of rough lemon. *Agronomy Journal*, 52(9), 530–532. <https://doi.org/10.2134/agronj1960.00021962005200090013x>
- Ozturk, M., Sakcali, S., Guceci, S., & Tombuloglu, H. (2010). Boron and plants. In M. Ashraf, M. Ozturk, & M. Ahmad (Eds.), *Plant Adaptation and Phytoremediation*. Springer. [https://doi.org/10.1007/978-90-481-9370-7\\_13](https://doi.org/10.1007/978-90-481-9370-7_13)
- Pandey, P., Ge, Y., Stoerger, V., & Schnable, J. C. (2017). High throughput in vivo analysis of plant leaf chemical properties using hyperspectral imaging. *Frontiers in Plant Science*, 8. <https://doi.org/10.3389/fpls.2017.01348>
- Paz-Kagan, T., Schmilovitch, Z., Yermiyahu, U., Rapaport, T., & Sperling, O. (2020). Assessing the nitrogen status of almond trees by visible-to-shortwave infrared reflectance spectroscopy of carbohydrates. *Computers and Electronics in Agriculture*, 178, 105755. <https://doi.org/10.1016/j.compag.2020.105755>
- Pech, J. M., Stevens, R. M., Grigson, G. J., Cox, J. W., & Schrale, G. (2013). Screening the Vitis genus for tolerance to boron with and without salinity. *Australian Journal of Grape and Wine Research*, 19(3), 446–456. <https://doi.org/10.1111/ajgw.12038>
- Penuelas, J., Baret, F., & Filella, I. (1995). Semi-empirical indices to assess carotenoids/chlorophyll a ratio from leaf spectral reflectance. *Photosynthetica*, 31(2), 221–230.
- Pereira, G. L., Siqueira, J. A., Batista-Silva, W., Cardoso, F. B., Nunes-Nesi, A., & Araújo, W. L. (2021). Boron: More than an essential element for land plants? *Frontiers in Plant Science*, 11. <https://doi.org/10.3389/fpls.2020.610307>
- Prananto, J.A., Minasny, B., & Weaver, T. (2020). Near infrared (NIR) spectroscopy as a rapid and cost-effective method for nutrient analysis of plant leaf tissues. *Advances in Agronomy*, 164, 1-49. <https://doi.org/10.1016/bs.agron.2020.06.001>
- Princi, M. P., Lupini, A., Araniti, F., Longo, C., Mauceri, A., Sunseri, F., & Abenavoli, M. R. (2016). Boron toxicity and tolerance in plants. In *Plant Metal Interaction* (pp. 115–147). Elsevier. <https://doi.org/10.1016/B978-0-12-803158-2.00005-9>
- Quartacci, M. F., Ranieri, A., & Sgherri, C. (2015). Antioxidative defence mechanisms in two grapevine (*Vitis vinifera* L.) cultivars grown under boron excess in the irrigation water. *Vitis*, 54(2), 51–58.
- R Core Team. (2024). R: A language and environment for statistical computing. R Foundation for Statistical Computing, Vienna, Austria. <https://www.R-project.org/>
- Riaz, M., Kamran, M., El-Esawi, M. A., Hussain, S., & Wang, X. (2021). Boron-toxicity induced changes in cell wall components, boron forms, and antioxidant defense system in rice seedlings. *Ecotoxicology and Environmental Safety*, 216, 112192. <https://doi.org/10.1016/j.ecoenv.2021.112192>
- Roberts, D. A., Roth, K. L., Wetherley, E. B., Meerdink, S. K., & Perroy, R.L. (2018). Hyperspectral vegetation indices. In *hyperspectral indices and image classifications for agriculture and vegetation* (2nd ed.). CRC Press. <https://doi.org/10.1201/9781315159331-1>
- Sah, R. N., & Brown, P. H. (1997). Techniques for boron determination and their application to the analysis of plant and soil samples. *Plant and Soil*, 193(1), 15–33. <https://doi.org/10.1023/A:1004251606504>
- Sarić, R., Nguyen, V. D., Burge, T., Berkowitz, O., Trtílek, M., Whelan, J., Lewsey, M. G., & Čustović, E. (2022). Applications of hyperspectral imaging in plant phenotyping. *Trends in Plant Science*, 27(3), 301–315. <https://doi.org/10.1016/j.tplants.2021.12.003>
- Sharma, S., Wong, C., Bhattarai, K., Lupo, Y., Magney, T., & Diaz-Garcia, L. (2024). Hyperspectral sensing for high-throughput chloride detection in grapevines. *The Plant Phenome Journal*, 7(1), e70012. <https://doi.org/10.1002/ppj2.70012>
- Shelp, B. J., Marentes, E., Kitheka, A. M., & Vivekanandan, P. (1995). Boron mobility in plants. *Physiologia Plantarum*, 94(2), 356–361. <https://doi.org/10.1111/j.1399-3054.1995.tb05323.x>
- Singh, A., Ganapathysubramanian, B., Singh, A. K., & Sarkar, S. (2016). Machine Learning for High-Throughput Stress Phenotyping in Plants. *Trends in Plant Science*, 21(2), 110–124. <https://doi.org/10.1016/j.tplants.2015.10.015>
- Uarrotta, V. G., Stefen, D. L. V., Leolato, L. S., Gindri, D. M., & Nerling, D. (2018). Revisiting carotenoids and their role in plant stress responses: From biosynthesis to plant signaling mechanisms during stress. In D. K. Gupta, J. M. Palma, & F. J. Corpas (Eds.), *Antioxidants and antioxidant enzymes in higher plants* (207–232). Springer International Publishing. [https://doi.org/10.1007/978-3-319-75088-0\\_10](https://doi.org/10.1007/978-3-319-75088-0_10)
- Wakuta, S., Fujikawa, T., Naito, S., & Takano, J. (2016). Tolerance to excess-boron conditions acquired by stabilization of a BOR1 variant with weak polarity in Arabidopsis. *Frontiers in Cell and Developmental Biology*, 4. <https://doi.org/10.3389/fcell.2016.00004>
- Walker, H.V., Jones, J.E., Swarts, N.D., Rodemann, T., Kerslake, F., & Damberg, R.G. (2021). Predicting grapevine canopy nitrogen status using proximal sensors and near-infrared reflectance spectroscopy. *Journal of Plant Nutrition and Soil Science*, 184, 204–304. <https://doi.org/10.1002/jpln.202000320>
- Wang, Y. M., Ostendorf, B., & Pagay, V. (2023). Detecting grapevine virus infections in red and white winegrape canopies using proximal hyperspectral sensing. *Sensors*, 23(5), Article 5. <https://doi.org/10.3390/s23052851>
- Warrington, K. (1923). The effect of boric acid and borax on the broad bean and certain other plants. *Annals of Botany*, 37(148), 629–672. <https://doi.org/10.1093/oxfordjournals.aob.a089871>
- White, P. J., & Broadley, M. R. (2001). Chloride in soils and its uptake and movement within the plant: A review. *Annals of Botany*, 88(6), 967–988. <https://doi.org/10.1006/anbo.2001.1540>
- Yermiyahu, U., Ben-Gal, A., & Sarig, P. (2006). Boron toxicity in grapevine. *HortScience*, 41(7), 1698–1703. <https://doi.org/10.21273/HORTSCI.41.7.1698>
- Yu, K., Anderegg, J., Mikaberidze, A., Karisto, P., Mascher, F., McDonald, B. A., Walter, A., & Hund, A. (2018). Hyperspectral Canopy sensing of wheat septoria tritici blotch disease. *Frontiers in Plant Science*, 9. <https://doi.org/10.3389/fpls.2018.01195>